Design Oriented Aerodynamic Modelling of Wind Turbine Performance

2007 J. Phys.: Conf. Ser. 75 012011

(http://iopscience.iop.org/1742-6596/75/1/012011)

Journal of Physics: Conference Series **75** (2007) 012011 doi:10.1088/1742-6596/75/1/012011

Design Oriented Aerodynamic Modelling of Wind Turbine Performance

Luca Greco[1], **Claudio Testa**[1], **and Francesco Salvatore**[1]

[1]INSEAN, Via di Vallerano, 00128 Rome, Italy

E-mail: f.salvatore@insean.it

Abstract. The development of a wind turbine aerodynamics model using a Boundary Integral Equation model (BIEM) is presented. The methodology is valid to study inviscid unsteady flows around three dimensional bodies of arbitrary shape and arbitrarily moving with respect to the incoming flow. The extension of this methodology to study viscosity effects in turbine blade flow at high angle of attack is addressed and an approach to determine aerodynamic loads over a wide range of turbine operating conditions is proposed. Numerical applications considering a selected test cases from the NREL experimental dataset are presented. Finally, the application of the proposed turbine aerodynamics model into a multi-disciplinary study including aeroelasticity of pylon-turbine assembly and aeroacoustics modelling of induced noise is briefly described.

1. Introduction

The effectiveness of a wind turbine plant is largely based on the capacity of rotor blades to extract energy from the incoming wind under given reliability, sustainability and safety standards. Among design challenges a careful selection of aerodynamics models used to describe the interaction between the rotor and the incoming flow is then of primary importance.

Flow features affecting the response of turbine blades to the incoming wind are the result of a complex interplay among three-dimensional flow effects, viscosity-induced separation and stall. Modelling the flowfield is further complicated by the necessity to take into account different sources of unsteadiness; non-uniformity of wind velocity profile, operation at yaw angles, shadow effect due to pylon in case of downwind layouts, is only an incomplete list of aspects making unsteady aerodynamics models necessary to describe wind turbine performance under real-life operating conditions.

Ongoing research topics clearly reflect the huge effort to address all the above aspects and to develop reliable analysis and design tools. A review of the variety of existing models to study wind turbine fluid-dynamics reveals that two major classes of approaches can be identified: *(i)* approximated two-dimensional inviscid-flow models including corrections to take into account three-dimensional effects and viscosity effects, and *(ii)* complex three-dimensional viscous-flow models based on the numerical solution of the Navier-Stokes equations.

Blade Element Models (BEM) and Reynolds-Averaged Navier-Stokes (RANS) methods represent the most popular approaches falling respectively within the two classes above.

A vast literature describes drawbacks and advantages of those methodologies (see, *e.g.,* [1] and [2]). Limiting to consider methods capable to provide realistic global performance predictions at reduced computational effort, the current trend is still to give preference to BEM-based

approaches, whereas more sophisticated RANS or other viscous-flow codes are used for 2D simulations or to focus on local analysis of rotating blade flow.

In the present paper, a performance prediction method is proposed that hardly can be grouped into any of the two classes above. The theoretical and computational methodology here proposed is based on a general formulation to describe the unsteady, three-dimensional flow around bodies of arbitrary shape immersed in a non-uniform inflow. The mathematical model is based on the assumptions of inviscid, incompressible flow, and hence viscosity effects are neglected and require suitable modelling.

Theoretical models of this type are widely used to study fluid-solid interaction of rotary-wings for aircraft as well as seacraft applications. The capability to describe strong three-dimensional flow effects as well as unsteady flow effects typical of helicopter rotor blades or marine propellers is clearly demonstrated. Recent work by the authors in these areas is described *e.g.,* in [3] and [4], whereas the application to the hydrodynamic analysis of vertical axis tidal turbines is described in [5]. This methodology is known among the aerodynamicists and hydrodynamicists communities as Boundary Element Methodology, and the acronym B.E.M is used: in order to avoid confusion with Blade Element Models, the alternative terminology Boundary Integral Equation Method (BIEM) will be used here.

Aim of this work is to extend an existing BIEM to study wind turbine performance. The appeal of this methodology is that three-dimensional and unsteady inviscid-flow effects are naturally taken into account, and no extra modelling is necessary to describe the attached flow over a blade surface free of viscous separation. This represents an important enhancement with respect to standard BEM models, where in addition to viscous loads corrections, three-dimensional and unsteady flow corrections are also introduced through approximated formulations that typically result into cumbersome algorithms that depend on semi-empirical models and non-physical parameters.

Using BIEM, additional modelling is limited only to describe viscosity effects that have a large impact on loads generated on blade sections at high angle of attack, under stall and post-stall conditions. The discussion of different strategies to face this problem is a major part of the present paper. The ultimate objective is to develop an approach that is as much as possible independedent of semi-empirical corrections.

In the following sections, the proposed theoretical formulation to study wind turbine flow using a BIEM is illustrated. The implementation of the mathematical model into a computational code is also briefly described. Moreover, a preliminary validation of the methodology is presented by considering a well-known test case from NREL/NASA Ames [6]. Numerical predictions of uniform, axial turbine flow and rotor performance are compared to experimental data.

The development of the blade aerodynamics BIEM model here described represents the first phase of a multi-disciplinary research program addressing wind turbines analysis and design. Objective of the research program is to realize a computational suite for the integrated analysis of aerodynamics, aeroelasticity, and aeroacoustics issues related to wind turbines operation. The capability of the proposed blade aerodynamics model to provide an adequate input for a large class of multi-disciplinary studies are briefly addressed in the conclusions.

2. Turbine aerodynamic loads modelling

The core of the turbine aerodynamics model proposed in this paper is based on inviscid flow assumptions, as it will be clarified in the next section. Here, the proposed approach to include viscosity-induced effects to aerodynamic loads is illustrated.

In general terms, force $\mathbf{f}$ and moment $\mathbf{m}_0$ exerted by a fluid on a solid body are obtained integrating normal and tangential stresses over the body surface $\mathcal{S}_B$ (in the present case of a

wind turbine, the body surface $\mathcal{S}_B$ identifies the overall surface of all turbine blades)

$$\mathbf{f} = \oint_{\mathcal{S}_B} (p\mathbf{n} + \tau\mathbf{t})\, d\mathcal{S}; \qquad \mathbf{m}_0 = \oint_{\mathcal{S}_B} [p(\mathbf{x}-\mathbf{x}_0)\times\mathbf{n} + \tau(\mathbf{x}-\mathbf{x}_0)\times\mathbf{t}]\, d\mathcal{S}, \tag{1}$$

where pressure p and friction τ represent respectively, normal and tangential stresses, acting on $\mathcal{S}_B$, and $\mathbf{n}, \mathbf{t}$ are unit vectors normal and tangential to $\mathcal{S}_B$ itself. Denoting by $\mathbf{e}_x$ a unit vector aligned to the turbine rotor axis, turbine thrust and torque are easily obtained as $T = \mathbf{f}\cdot\mathbf{e}_x$ and $Q = \mathbf{m}_0\cdot\mathbf{e}_x$, respectively.

Consider the aerodynamic force $\mathbf{f}$. Under attached flow conditions, pressure is unaffected by viscosity and hence the first term in the right-hand side of Eq. 1 can be accurately described under inviscid 3D-flow assumptions. A simple boundary layer flow solver can be used to estimate τ and then to determine viscous-flow contributions to blade loads (see, *e.g.,* [7] where coupling of BIEM with a boundary layer solver is applied to study marine propeller flows).

Unfortunately, attached flow conditions on wind turbine blades occour only over a limited range of operational conditions. In case of separated flow as trailing edge separation, stall and post-stall conditions, pressure is largely dominated by viscosity, and 3D-flow effects have a strong influence on the development of separated flow regions on blade (see, *e.g.,* [1]). Under these flow conditions, pressure can be formally decomposed into $p = p_{pot} + \Delta p_{vis}$, where Δp_{vis} represents the correction of inviscid-flow pressure p_{pot} due to viscosity effects.

Considering this pressure decomposition into the first of Eqs. 1, yields

$$\mathbf{f} = \mathbf{f}_{pot} + \mathbf{f}_{vis} = \oint_{\mathcal{S}_B} p_{pot}\mathbf{n} d\mathcal{S} + \oint_{\mathcal{S}_B} (\Delta p_{vis}\mathbf{n} + \tau\mathbf{t})\, d\mathcal{S}. \tag{2}$$

The first integral in the right-hand side, $\mathbf{f}_{pot}$, can be evaluated using the inviscid 3D-flow model. The second integral represents the unknown contribution due to viscosity: the rest of this section is devoted to modelling this quantity, hereafter referred to as *3D viscous correction*, $\mathbf{f}_{vis}$.

The approach proposed here to evaluate quantity $\mathbf{f}_{vis}$ is based on a partial analogy between a turbine blade section at arbitrary location s along span and a two-dimensional profile of identical shape. The quantity $\mathbf{f}_{vis}$ may be determined as the integral of a spanwise distribution of blade load per unit span as $\mathbf{f}_{vis} = \int \mathbf{f}'_{vis}(s)ds$. Recalling in two dimensions profile loads are typically expressed in terms of lift and drag components, it is convenient to use the following expression of the 3D viscous correction per unit span

$$\mathbf{f}'_{vis}(s) = \oint_{C(s)} (\Delta p_{vis}\mathbf{n} + \tau\mathbf{t})\, dl = \Delta L^{3D}_{vis}(s)\mathbf{e}_n + D^{3D}_{vis}(s)\mathbf{e}_t, \tag{3}$$

where $\mathbf{e}_t$ is a unit vector parallel to the local inflow direction and $\mathbf{e}_n$ is normal to it, ΔL^{3D}_{vis} is the viscous correction to local lift and D^{3D}_{vis} denotes viscous drag.

The key of the present approach is to assume that sectional viscous lift ΔL^{3D}_{vis} and drag D^{3D}_{vis} are identical to those of a two dimensional profile at 'equivalent' angle of attack, α_{eq}. The equivalent angle of attack is determined simply imposing that the total lift of the 3D sectional profile equals the total potential lift of the 2D profile.

Assuming two-dimensional lift and drag L^{2D}, D^{2D} are given (see comments below), the following procedure is used to determine the equivalent angle of attack α_{eq}, and hence quantities ΔL^{3D}_{vis}, D^{3D}_{vis} (see Fig. 1):

(i) determine the distribution along blade span of $L^{3D}_{pot}(s, \alpha(s))$ from inviscid-flow calculations;

(ii) impose at each spanwise location s: $L^{3D}_{pot}(s, \alpha(s)) \equiv L^{2D}_{pot}(s, \alpha_{eq}(s))$ to determine $\alpha_{eq}(s)$;

(iii) evaluate $\Delta L^{3D}_{vis} = L^{3D}_{pot} - L^{2D}$ and $D^{3D}_{vis} = D^{2D}$.

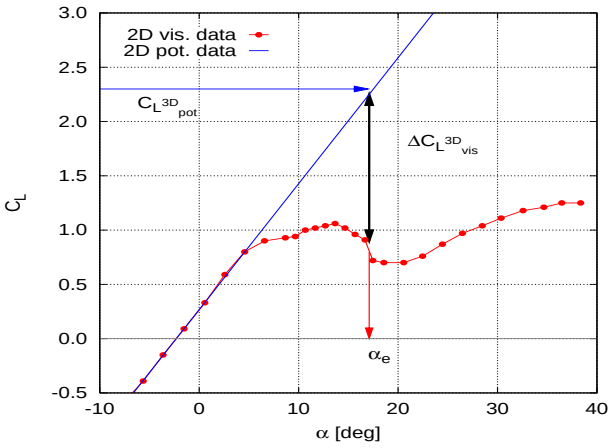

Figure 1. Lift and drag characteristics of the S809 airfoil: 2D potential and viscous data used for the α_{eq} correction.

Once viscous contributions to blade loads are estimated, global turbine thrust and torque can be determined using Eq. 2 for $\mathbf{f}$ and a similar relationship for $\mathbf{m}_0$. This proposed methodology will be addressed in the following as BIEM-α approach.

The proposed approach may be commented noting that three-dimensional attached flow effects around rotating blades are described without any approximation. Viscous flow correction is straightforward and does not rely on semi-empirical relationships based on critical tuning of problem-dependent parameters. In input, the proposed approach requires lift and drag characteristics of the two dimensional profiles describing blade section. Here it is assumed that this information can be derived by experimental data or by numerical analysis using 2D viscous-flow solvers.

The only assumption made is that viscosity effects acting on each blade section can be estimated from an equivalent two-dimensional flow. Of course, consequences of such an assumption require a careful assessment, as it will be described in the following sections. In particular, the possibility to describe the well-known delay of separated flow effects in three dimensional flows on rotating blades needs to be investigated.

The proposed viscous correction model is developed under steady flow conditions. Suitable modelling of unsteady inflow (non zero yaw angle of attack, non uniform wind speed, etc.) and dynamic stall phenomena will be addressed in the next phases of the research programme.

3. Derivation of the turbine aerodynamics model

At this stage it is worthy observing that the knowledge of the 3D unsteady aerodynamic blade loads is fundamental to characterize the behaviour of the wind–turbine with respect to aeroelastic and aeroacoustic applications (see *e.g.*[8], [9] and [10]). In fact, such loads are the forcing terms of the equations of the blade motion that yield the aeromechanical response of the system, and represent an acoustic source forcing the wave equation that governs the pressure disturbance radiated from the blade to the flow–field. Hence the capability to model the loads disribution on the blade surface in a physically consistent way, deeply affects the prediction of the performances of the turbine from an aeroacoustoelastic standpoint. The proposed aerodynamics model, described in this section, is characterized by a good compromise between accuracy and computational costs and is well suited to aeroacustoelastic coupling.

A general BIEM formulation for the analysis of the inviscid three-dimensional flow around bodies of arbitrary shape and in arbitrary motion is briefly outlined in this section. Details are omitted here and may be found in [3] and [7].

3.1. BIEM formulation for inviscid flow

Assuming the inflow to the turbine is inviscid and initially irrotational, the flow perturbation induced by the blades is irrotational and hence it may be described by a potential velocity field such that $\mathbf{v} = \nabla\varphi$ where φ is a scalar potential.

Considering the flowfield around a multi-blade rotor in an arbitrary axial inflow, the total velocity field at an arbitrary point $\mathbf{x}$ is then expressed in a frame of reference fixed to the rotating blades (RFR) as

$$\mathbf{q} = \nabla\varphi + \mathbf{v}_I = \nabla\varphi + 2\pi n\hat{\mathbf{x}}_R \times \mathbf{r} + \mathbf{R}_{FR}\mathbf{v}_w \tag{4}$$

where $\mathbf{r} = \mathbf{x} - \mathbf{x}_0$, $\mathbf{x}_0$ is the origin of RFR and $\mathbf{R}_{FR}$ is the rotation matrix from the fixed frame of reference to RFR. The quantity $\mathbf{v}_I$ represents the inflow to the blade given as the sum of the incoming wind $\mathbf{v}_w$ and the tangential velocity due to the blade rotation about the turbine shaft.

Recalling potential field theory, the continuity equation for the perturbation velocity of an incompressible inviscid fluid simply reduces to the Laplace equation for the velocity potential

$$\nabla^2\varphi = 0 \tag{5}$$

Under the same assumptions, the momentum equation is recast into the Bernoulli Equation, relating the velocity potential and pressure

$$\frac{\partial\varphi}{\partial t} + \frac{1}{2}q^2 + \frac{p}{\rho} + gz_0 = \frac{1}{2}v_I^2 + \frac{p_0}{\rho} \tag{6}$$

where p is the pressure, $q = \|\mathbf{q}\|$, $v_I = \|\mathbf{v}_I\|$, whereas g is the gravity acceleration and z_0 denotes is the vertical distance from a reference location.

A classical derivation, yields a solution of the Laplace equation 5 in terms of the following boundary integral formulation:

$$E(\mathbf{x})\varphi(\mathbf{x}) = \sum_{i=1}^{Z} \oint_{\mathcal{S}_{B_i}} \left(\frac{\partial\varphi}{\partial n}G - \varphi\frac{\partial G}{\partial n}\right) d\mathcal{S}(\mathbf{y}) + \sum_{i=1}^{Z} \int_{\mathcal{S}_{W_i}} \Delta\varphi\frac{\partial G}{\partial n} d\mathcal{S}(\mathbf{y}) \tag{7}$$

where Z is the number of blades, $\mathcal{S}_{B_i}$ is the surface of the $i-th$ blade, whereas $\mathcal{S}_{W_i}$ denotes the surface of the wake generated by the $i-th$ blade. The quantity $\mathbf{n}$ is the unit normal to $\mathcal{S}_{B_i}$ and to $\mathcal{S}_{W_i}$, and $G = -1/4\pi\|\mathbf{x} - \mathbf{y}\|$ denotes the unit source in the unbounded three-dimensional space. In addition, $E(\mathbf{x})$ equals 0, $\frac{1}{2}$, 1 if $\mathbf{x}$ is, respectively, inside, on or outside the rigid blades. The above integral formulation allows to predict the velocity potential everywhere in the flow–field once the potential distribution upon the blade(s) and $\Delta\varphi$ on the potential wake(s) are known. Hence, by approaching $\mathbf{x}$ to the body surface, Eq. 7 transforms into a boundary integral equation for φ that is solved imposing suitable boundary conditions on the body and wake surfaces.

On the blade surfaces the impermeability condition yields $\mathbf{q}\cdot\mathbf{n} = 0$, or, recalling Eq. 4,

$$\frac{\partial\varphi}{\partial n} = -\left(2\pi n\hat{\mathbf{x}}_R \times \mathbf{r} + \mathbf{R}_{FR}\mathbf{v}_w\right)\cdot\mathbf{n} \qquad \text{on } \mathcal{S}_{B_i} \tag{8}$$

In the framework of potential field theory, it may be proved that the trailing wakes $\mathcal{S}_{W_i}$ correspond to discontinuity surfaces for the velocity potential. Mass and momentum conservation laws are imposed across $\mathcal{S}_{W_i}$ to obtain that both pressure and the normal component of the perturbation velocity $\partial\varphi/\partial n$ are continuous:

$$\Delta p = 0; \qquad \Delta\left(\frac{\partial\varphi}{\partial n}\right) = 0; \qquad \text{on } \mathcal{S}_{W_i} \tag{9}$$

where Δ denotes discontinuity across the wake surface.

Combining the Bernoulli Eq. 6 and $\Delta p = 0$, one obtaines that $\Delta\varphi$ is constant following wake particles

$$\Delta\varphi\left(\mathbf{x},t\right) \;=\; \Delta\varphi\left(\mathbf{x}_{_{TE}},t-\tau_{_W}\right) \qquad \text{on } \mathcal{S}_{_{W_i}} \tag{10}$$

where $\mathbf{x}_{_{TE}}$ is a wake point at the blade trailing edge and $\tau_{_W}$ denotes the convection time of particles moving on the wake surface with velocity $\mathbf{v}_{_I}$. An additional condition on φ is required in order to assure that no finite pressure jump may exist at the body trailing edge (Kutta condition). This condition is approximately achieved by imposing that $\Delta\varphi$ at the wake trailing edge equals the difference between potentials at the two sides of the blade trailing edge surface.

A simple and approximated representation of the wake surfaces is obtained by assuming for $\mathcal{S}_{_{W_i}}$ an helical surface (*prescribed wake modeling*). In spite of its semplicity such a kind of modeling may provide an unrealistic description of the trailing vorticity convection, depending both on the blade geometry and operating conditions. Alternatively, a physically–consistent wake shape may be determined imposing that wake points must be alligned to the local induced flow field downstream the blades. This nonlinear procedure is labelled as *wake alignment technique* [3] and allows to determine the wake shape as a part of the potential flow solution.

The solution of the integral equation for the velocity potential coupled with Bernoulli equation allows the evaluation of the pressure distribution p_{pot} in eq. 2 over the blade.

4. Numerical applications: the NREL/NASA Ames test case

The development of CFD tools to describe wind turbine aerodynamics can rely on an impressive amount of experimental data derived both from field measurements on full scale plants and from dedicated model tests. A preliminary validation of numerical results by the aerodynamic model described above has been performed considering comparison data from the Phase VI of the NREL/NASA Ames wind tunnel test. This experimental dataset is described in [6] and, despite the design constraints due to scientific needs, the analyzed system is representative of modern commercial wind turbines.

For the present validation excercise, a 10.58 m diameter two-bladed turbine rotor in axial uniform flow has been considered (upwind S configuration). Blade shape is characterized by a $S809$ airfoil with linear chord distribution and non-linear twist spanwise (see Fig. 2). A constant pitch value of 3° is considered and the blade cone angle is set to 0°. Further details on the rotor mechanical and geometrical characteristics can be found in [6] and [11].

Although the present aerodynamic BIEM-based model allows to study three-dimensional bodies of complex shape, here a simplified turbine model without rotor hub and pylon is accounted for. The integral equation for the velocity potential described above is solved by discretizing the rotor blades and trailing wakes surfaces into non-planar hyperboloidal quadrilateral elements. Computational grids are characterized by the number of blade elements in chordwise direction $M_B/2$ (from leading edge to trailing edge) and in spanwise direction N_B, the number of wake elements in streamwise direction per turn M_W and in radial direction N_W. Flow quantitites are supposed to be piecewise constant on each element. The boundary integral equation is enforced at each element centroid on the body surface, and hence its solution is reduced to the solution of a linear system of equations.

In order to provide an adequate description of blade flow, two distinct portions of each blade are considered, as depicted in Fig. 2. The inner part of the NREL blade (black-coloured grid, 10% of span) is characterized by transition from cylindrical sections close to hub to streamlined sections where $S809$ airfoil sections are used (red-coloured grid). This portion of the blade close to hub provides a minor contribution to aerodynamic loads and is modelled here as a non-lifting body. The remaining portion of the blade, from 10% to full span has $S809$ profile sections and

represents the lifting blade portion. The trailing wake associated to blade lift generation is thus emanated only from this latter blade portion. In Fig. 2 a helicoidal trailing wake determined through a simple analytical model is depicted. The influence of the trailing wake modelling on the performance predictions will be discussed later.

A peculiar aspect of the proposed BIEM approach is the capability to describe three–dimensional flow features. An example of this is given by Fig. 3, where pressure distribution over the blade surface determined from Eq. 6 is depicted. In addition to typical trends on airfoils, *i.e.,* strong pressure defect at the leading edge on the suction side, high pressure gradients in the spanwise direction are apparent on both blade pressure and suction sides.

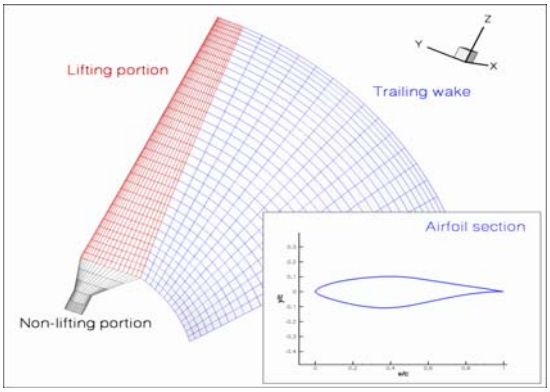

Figure 2. NREL blade: example of computational grid and geometrical characteristics

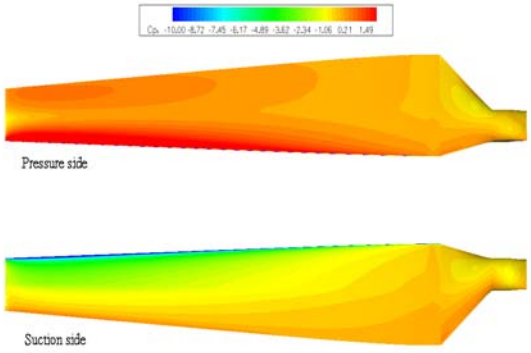

Figure 3. NREL blade: pressure distribution (p_{pot}) evaluated by BIEM approach.

As a preliminary assessment of numerical predictions, numerical scheme consistency, *i.e.,* the effect of grid refinement on $\mathcal{S}_B$ and $\mathcal{S}_W$, and the extension of wake surface considered in calculations, has been analyzed. Results of these analyses are summarized in Table 1, where measured thrust and torque from [6] are used for reference. Discrepancies between numerical predictions and measurements are generally reduced as discretization grid size is increased. Similar results are obtained by increasing the extension of the trailing wake.

N_{grid}	107	139	169	199	227
$100 \cdot (K_T^{num} - K_T^{exp})/K_T^{exp}$	10,48	9,35	9,10	9,03	8,99
$100 \cdot (K_Q^{num} - K_Q^{exp})/K_Q^{exp}$	19,66	25,94	22,52	19,83	18,19
N_{turns}	2	3	4	5	6
$100 \cdot (K_T^{num} - K_T^{exp})/K_T^{exp}$	9,75	9,03	8,73	8,59	8,50
$100 \cdot (K_Q^{num} - K_Q^{exp})/K_Q^{exp}$	21,14	19,83	19,29	19,03	18,88

Table 1. Effect of discretization parameters on numerical BIEM predictions for NREL blade at $V_w = 7$ m/s. (BIEM, no α_{eq} correction applied). Symbol N_{turns} denotes number of wake spiral turns, and $N_{grid} = [(M_B + M_W * N_{turns}) * N_B]^{\frac{1}{2}}$.

Numerical results are obtained using discretization parameters resulting from a trade-off between computational effort and sensitivity of results with respect to further grid refinements. Specifically, $M_B = 180, N_B = 55, N_{grid} = 199$, and $N_{turns} = 3$ grids are used here. With the present non–optimized code, the numerical simulation of rotor performance for a single operating condition requires about 20 minutes on a Pentium IV pc with a single–core 3.0 GHz processor.

One of the aspects to be carefully investigated in the aerodynamic analysis of wind turbines is whether the blades (or blade portions) are operating under attached or separated flow conditions. The capability of the proposed BIEM and BIEM-α approaches to describe turbine loads under those different flow conditions is of primary importance for design applications.

The occurrence of attached or separated blade flow conditions is largely dominated by the actual distribution of blade angle of attack. In particular, the kinematic angle of attack α_{kin} results from a combination of incoming wind speed, blade rotational speed and blade geometrical characteristics, and does not take into account for the rotor-induced perturbation velocity.

Figure 4 depicts the spanwise distribution of the NREL blade angle of attack under different wind speed conditions. Numerically evaluated α_{kin} is compared to measured data obtained with five-hole pressure probes. The numerical model reproduces the observed blade motion with good agreement; some minor discrepancies are found near the blade root where an influence of the wake of the instrumentation boom mounted upwind the turbine is expected.

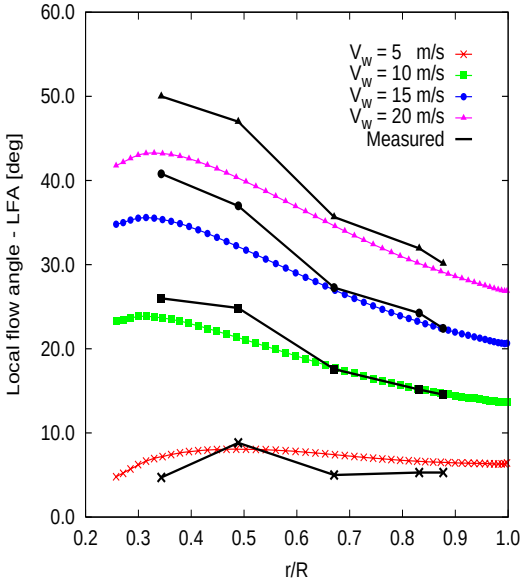

Figure 4. Kinematics of the NREL rotor blade: predicted local flow angle compared to measured values from [6].

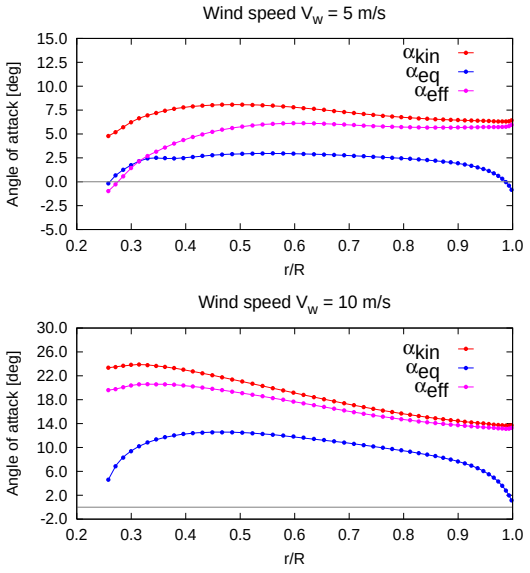

Figure 5. Predicted sectional angle of attack (AoA): local flow angle (α_{kin}), effective AoA (α_{eff}), equivalent AoA (α_{eq}).

Basing on the kinematic angle of attack, the effective angle of attack α_{eff} accounting for the induced velocity field may be evaluated. The numerical calculation of α_{eff} using a simple model based on blade element theory for a rotor with twisted and tapered blades in axial climb (see [12]) is presented in Fig. 5, where the NREL blade at 1.2 rps and $V_w = 5$ m/s, $V_w = 10$ m/s, respectively, is considered. Comparing distributions of α_{kin} and α_{eff}, it follows that the effect of induced velocity is to reduce the spanwise distribution of the angle of attack.

Combining α_{eff} results in Fig. 5 and experimental 2D $C_L - \alpha$ and $C_D - \alpha$ curves from Fig. 1, yields that more than 50% of the blade span should be stalled for $V_w = 5$ m/s whereas fully separated flow conditions should occur for $V_w = 10$ m/s. This is in contrast to experimental evidencies that stall onset occours only at V_w larger than 10 m/s. In fact, applying the procedure in Section 2 to determine the equivalent angle of attack α_{eq}, the results in Fig. 5 show that blade sections are working under *equivalent* 2D conditions at lower angle of attack than both α_{kin} and α_{eff}. This provides a physical explanation of the meaning of quantity α_{eq} introduced in the present work.

Once sectional viscous contributions to blade loads are estimated, total sectional loads (potential plus viscous correction) may be calculated in terms of normal and tangential components with respect to local chord. Figure 6 depicts the radial distribution of tangential and normal force coefficients along the blade at $V_w = 7$ m/s and $V_w = 10$ m/s. Numerical predictions by BIEM are compared to distributions evaluated using the α_{eq} correction (BIEM-α) and to measurements. Using inviscid flow BIEM, force coefficients are over–predicted thus indicating that viscosity induced effects are relevant even at relatively low wind speeds. In fact, loads estimation based on the inclusion of the α_{eq} correction clearly improves numerical predictions at $V_w = 7$ m/s. For larger wind speed ($V_w = 10$ m/s), BIEM-α-based estimations are still accurate throughout blade span except at inner blade sections where high angle of attack causes stall onset, as shown by the dip in the tangential force coefficient (Figs. 6, bottom right).

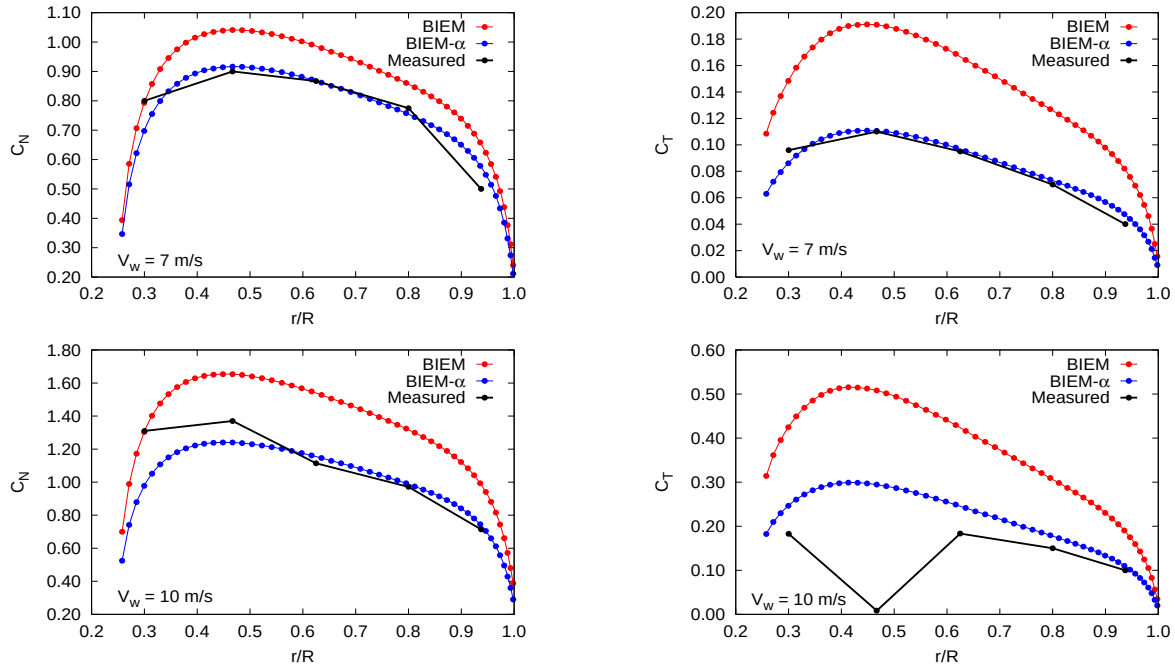

Figure 6. Normal (left) and tangential (right) force coefficient: numerical BIEM and BIEM-α calculations compared to experiments from [6]. Top: $V_w = 7$ m/s; bottom: $V_w = 10$ m/s.

Next, predictions of turbine rotor aerodynamic loads at different wind speeds are presented in Fig. 7. Experimental data are compared to numerical predictions using both BIEM and BIEM-α models. For reference, the PROPID code [11] based on the blade element/momentum theory, and 2D predictions obtained here using the effective angle of attack α_{eff} computed by a simple induced velocity approach by BEM are also considered. All these numerical approaches use as input the experimental 2D airfoil characteristics taken from [13] and [6].

Considering thrust, left Fig. 7 shows that BIEM provides a good estimate of turbine loads only up to 7 m/s, whereas the BIEM-α method improves the accuracy over a wind speed range up to 20 m/s. It is worth noting that at increasing wind speed, the present 2D aerodynamic model as well as PROPID code tend to underpredict rotor thrust.

The analysis of torque curve, right Fig. 7, shows that BIEM aerodynamic model is accurate only up to $V_w = 6$ m/s, whereas the α_{eq} correction yields improved results up to 8 m/s. Throughout that speed range, 3D BIEM-α methodology yields estimations more accurate than those obtained by the 2D BEM-based model, whereas PROPID predictions are sufficiently accurate for operating conditions up to stall onset ($V_w = 10$ m/s).

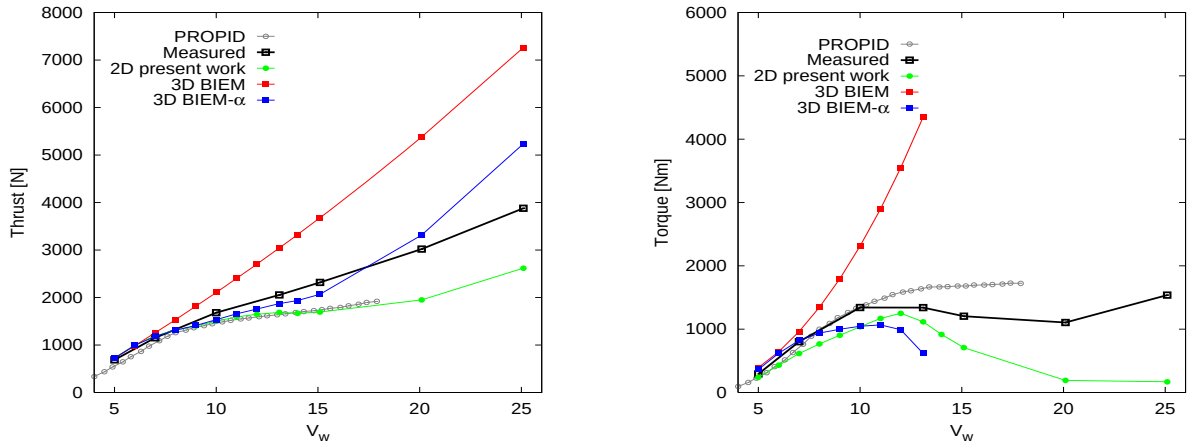

Figure 7. Thrust (left) and torque (right) curve predictions: measured data compared to different numerical methodologies.

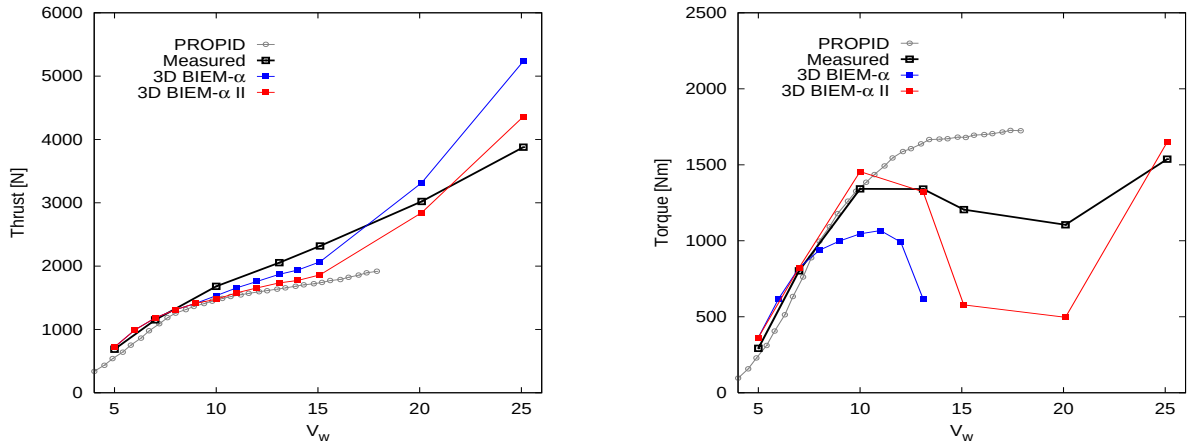

Figure 8. Influence of induced drag on thrust (left) and torque (right) predictions.

The assessment of the proposed BIEM and BIEM-α methodologies highlights that for low/medium wind speed, 3D–fully attached flow model (with the 'equivalent' α correction) is a useful tool to predict turbine performance. The behavior of the numerical solution indicates that blade aerodynamics is governed by velocity potential theory, and viscosity effects may be predicted with satisfactory accuracy through local angle of attack equivalence. Moreover, the region where turbine-generated thrust is reliably predicted by BIEM-α is extended to a range of operating conditions covering most of design needs. Nevertheless, electric power generation is related to aerodynamic torque that is more affected by lift–induced drag and viscosity effects than thrust. Numerical results show that the capability of the proposed BIEM-α approach in capturing such phenomena is quite satisfactory up to stall onset. Under massively separated flow conditions, BIEM-α approach tends to overestimate the viscosity effects causing an unrealistic decay of predicted torque (Fig. 7, right) with respect to measured data. This shortcoming is expected because of the inaccuracy of BIEM models in describing lift–induced drag at *high* angle of attack, *i.e.,* out of the linear range of the $C_L - \alpha$ curve.

Such considerations are confirmed by observing Fig. 8. Here, thrust and torque predictions by BIEM-α model are compared to those obtained by setting to zero the lift–induced drag for wind speed larger than 9 m/s (BIEM-α II approach). A marked improvement of predicted torque

is found in the range $V_w = 9-13$ m/s. Although the assumption under the BIEM-α II approach is not justified, this test provides a starting point for further investigations on a suitable way for modelling 3D separation phenomena in the framework of the BIEM-α methodology.

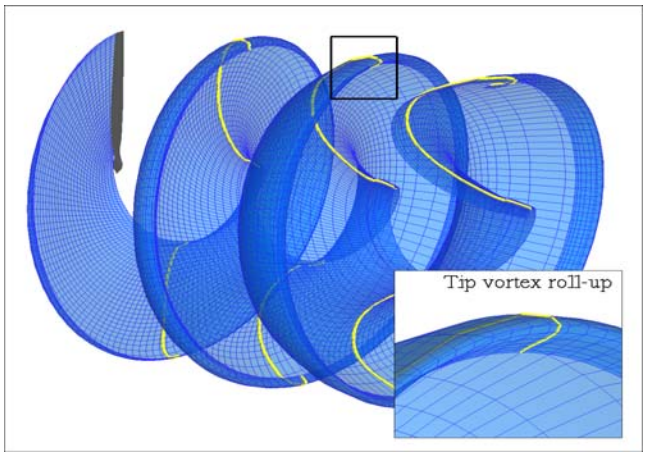

Figure 9. NREL blade: trailing wake shape predicted by BIEM using a wake alignment model. Three-dimensional view of rolled-up wake surface and close-up in the tip vortex region.

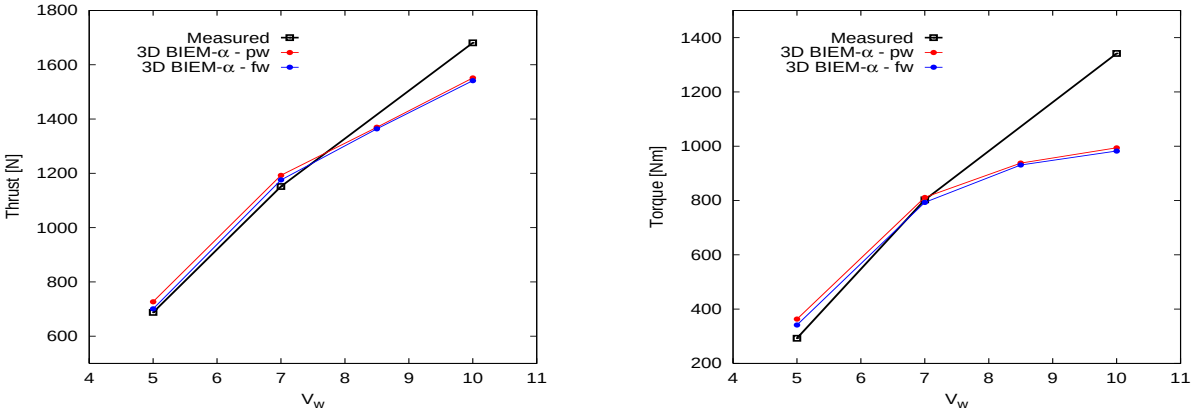

Figure 10. Influence of trailing wake modelling on thrust (left) and torque (right): BIEM-α predictions using flow-aligned wake and helicoidal wake models compared to measured data.

Finally, the influence of trailing wake shape on performance predictions has been investigated. A representative example of the calculated wake surface aligned to the local flow is shown in Fig. 9. The effect of capturing the real shape of the rotor wake in loads predictions is shown in Fig. 10. For wind speed up to 8.5 m/s, the agreement between measured and predicted thrust and torque is markedly improved if a flow-aligned wake is used instead of a simple helicoidal surface. For larger wind speed, where viscosity induced effects are dominating over potential governed phenomena, predicted loads are slightly affected by the two different wake shapes used.

5. Concluding remarks and future work

A wind turbine aerodynamics model based on a Boundary Integral Equation Method (BIEM) has been presented. Generally speaking, such methodology allows to describe the inviscid flow around three-dimensional bodies of arbitrary shape moving in arbitrary motion with respect to an incoming flow. For wind turbines, deeply affected by viscous effects, a novel formulation capable to account for such effects has been presented. A distinguishing feature of the proposed approach is that no semi-empirical relationships are required and the resulting implementation is straightforward. Numerical applications of the proposed methodology show that the estimation

of turbine performances is reliable up to stall onset. The introduction of a trailing wake alignement technique has shown to even improve the code reliability for that wind speed range.

For separated flow operating conditions, discrepancies with respect to experimental data occur. Hence, a more physically consistent way of accounting for viscous effects has to be considered. Similarly, some issues related with the corrected evaluation of lift–induced drag at high blade incidence have been identified and will the subject for further investigations.

The blade aerodynamics BIEM model here described, represents the result of the first phase of a multi-disciplinary research program addressing wind turbines analysis and design. Mid-term objective of the research program is to develop a computational suite for the integrated analysis of aerodynamics, aeroelasticity, and aeroacoustics issues related to wind turbines operation. It is worth to emphasize that the proposed aerodynamic methodology is suitable for describing the aerodynamic forcing terms when body elasticity is accounted for. In fact, the derivation of the aeroelastic operator through which the aeroelastic stability analysis and the aeroelastic response may be performed, is quite straighforward (see [8]). Furthermore, the present BIEM formulation is fully adeguate to provide aerodynamic input for aeroacoustic solvers capable to determine the aerodynamically generated noise (see [10]). Both aeroelastic and aeroacoustic issues represents the core of the future activity.

Acknowledgments

The authors wish to thank Mr. Scott Schreck for kindly providing access to information and data from the NREL/NASA Ames experimental dataset.

References

[1] Sørensen N N, Michelsen J A and Schreck S 2002 Navier–Stokes predictions of the NREL phase VI rotor in the NASA Ames 80 ft × 120 ft wind tunnel *Wind Energy* **5** 151–169

[2] Martinez J, Bernabini L, Probst O and Rodriguez C 2005 An improved BEM model for the power curve prediction of stall–regulated wind turbines *Wind Energy* **8** 385–402

[3] Greco L, Salvatore F and Di Felice F 2004 *Proceedings of the Twenty-fifth ONR Symposium on Naval Hydrodynamics* Validation of a quasi–potential flow model for the analysis of marine propellers wake, St. John's, Newfoundland (Canada)

[4] Greco L, Colombo C, Salvatore F and Felli M, 2006 *Proceedings of the TPOD 2006 - Second International Conference on Technological Advances in Podded Propulsion* An unsteady inviscid–flow model to study podded propulsors hydrodynamics, Brest, France

[5] Salvatore F, Greco L, Calcagno G, Moroso A and Eriksson H 2006 *Proceedings of the OWEMES 2006 Seminar on Offshore Wind and other Marine Renewable Energies in Mediterranean and European Seas* A theoretical and computational methodology to study vertical-axis turbines hydrodynamics, Civitavecchia, Italy

[6] Hand M M, Simms D A, Fingersh L J, Jager D W, Cotrell J R, Schreck S and Larwood S M 2001 *Unsteady aerodynamics experiment phase VI: wind tunnel test configuration and available data campaigns*, NREL/TP-500-29955, Golden (Colorado), USA

[7] Salvatore F, Testa C and Greco L 2003 *Proceedings of CAV 2003 Symposium* A viscous/inviscid coupled formulation for unsteady sheet cavitation modelling of marine propellers, Osaka, Japan

[8] Testa C, Leone S, Serafini J and Gennaretti M 2006 *Proceedings of the 32–th European Rotorcraft Forum* Aeroelastic investigation of hingeless helicopter blades with integrated morphing actuator, The Netherlands

[9] Gennaretti M, and Greco L 2005 *Proceedings of the International Forum on Aeroelasticity and Structural Dynamics - IFASD 2005* Unsteady aerodynamic reduced–order models for the analysis of proprotor whirl–flutter instability, Munich, Germany

[10] Testa C, Salvatore F, Ianniello S and Gennaretti M 2005 *Proceedings of the 11–th AIAA/CEAS Aeroacoustics Conference* Theoretical and numerical issues for hydroacoustics applications of the Ffowcs Williams-Hawkings equation, Monterey, California (USA)

[11] Giguère P and Selig M S 1999 *Design of a tapered and twisted blade for the NREL combined experiment rotor*, NREL/SR-500-26173, Golden (Colorado), USA

[12] Leishmann J G 2001 *Principles of helicopter aerodynamics* Cambridge University Press New York (USA)

[13] Reuss Ramsay R, Hoffmann M J and Gregorek G M 1995 *Effects of grit roughness and pitch oscillations on the S809 airfoil* , Airfoil performance report NREL/TP-442-7817, Golden (Colorado), USA